Angular regimes of ac dynamics and pinning in YBa$_2$Cu$_3$O$_7$ crystals with and without columnar defects

G. Pasquini,[1,*] L. Civale,[2] H. Lanza,[3] and G. Nieva[2]

[1]*Universidad de Buenos Aires, Departamento de Física, Facultad de Ciencias Exactas, Ciudad Universitaria, 1429, Buenos Aires, Argentina*
[2]*Comisión Nacional de Energía Atómica-Centro Atómico Bariloche and Instituto Balseiro-8400 Bariloche, Argentina*
[3]*Comisión Nacional de Energía Atómica-Departamento de Física, TANDAR, Buenos Aires, Argentina*

The main source of vortex pinning near the solid-liquid transition at different orientations of a low dc field in YBa$_2$Cu$_3$O$_7$ crystals with columnar defects is investigated by means of ac susceptibility measurements. The behavior is compared with that observed in nonirradiated samples. It is found that in a very wide angular region the tracks act as correlated defects and are the prevailing source of pinning. The results rule out the existence of an accommodation angle, determined by the competition between the pinning and elastic energies, in twined crystals: the interplay with natural correlated pinning centers has to be taken into account. The linear and nonlinear dynamic regimes when the field is tilted relative to the defects are analyzed. It is clearly shown that characterization of the dynamic regimes is crucial for the correct interpretation of the angular dependence in the ac response.

I. INTRODUCTION

Up to now, a great effort has been devoted to understand the interplay between the phase diagram of the vortex system in high-temperature superconductors (HTSC's), its dynamical regimes, and the underlying quenched disorder.[1] At present, it is well known that defect topology affects drastically both the dynamic and static behavior. In this framework, the phase diagram of the vortex system as well as its dynamics has been intensely studied in HTSC's with columnar defects (CD's) when the magnetic field H_{dc} is aligned with the tracks.[2–10] In this case, several facts have been established: There is a second-order phase transition at a temperature T_{BG} higher than the preirradiation melting temperature. Below this line, vortex matter freezes into a Bose-glass phase.[1,4–6] For low enough temperatures and fields, each vortex is pinned by a single track. This individual pinning regime holds below a line $B_{rb}(T)$. Above this boundary the intervortex interactions become significant and pinning turns collective. At low temperatures $B_{rb}(T)$ approaches the matching field B_ϕ (the field at which vortex and defects densities are the same). Above the "depinning temperature" T_{dp}, the line B_{rb} drops abruptly,[7,8] so that for high temperatures, the individual pinning regime is limited to a region of very low fields.

In previous papers we have investigated the dynamical ac response of the vortex system at high T, in a low density of correlated defects.[9,10] We have established that the response can be described, up to temperatures very close to T_{BG}, in terms of an equation of motion for the vortex system and we have built a quantitative dynamical diagram in the plane (h_a, T). For low amplitudes h_a of the ac field, a linear response with scarce dissipation, characteristic of the Campbell regime (in which the average vortex positions oscillate inside the pinning centers), holds. The curvature of the pinning potential wells (Labusch constant) results independent of B up to $H_{dc} \sim B_\phi/2$. For large enough ac fields, a critical-state regime with activation energies strongly dependent on T and J is established. In between both regimes, there is a large region (more than one order of magnitude in h_a) where there is a nonlinear response determined from both intra- and intervalley motion of the vortex system.

On the other hand, when defects are not aligned with H_{dc}, several questions are still open. In the initial works of Nelson and Vinokur,[4] *for a system containing a single set of parallel correlated defects*, the authors predicted the following scenario: when the angle between the applied field and CD's is small enough, vortices are expected to remain locked into the defects. For tilts larger than the lock-in angle φ_L, vortices are expected to form staircase structures with segments pinned into different defects and connected by unpinned or weakly pinned segments. For tilt angles beyond an accommodation angle φ_A, the simplest scenario states that vortices will be straight and take the direction determined by the applied field, thus being unaffected by the correlated nature of the pinning. The same qualitative description applies for the case of planar correlated disorder (e.g., twin boundaries). Theory also predicts that the accommodation angle decreases with increasing temperature, as the ratio between the pinning and elastic energies, and goes to zero when $T \to T_{BG}$.

More recently, however, several experiments have shown that the actual situation in twined YBa$_2$Cu$_3$O$_7$ crystals with columnar defects is more complex. This is a consequence of the interplay of the CD's with the natural sources of correlated pinning: namely, twin boundaries (TB's) and ab planes. The response, in this case, is not simply described by taking into account an accommodation angle for each direction of correlated defects. Measurements of the angular dependence of the irreversible magnetization established that the combined effect of the three sources of correlated pinning must be taken into account to describe the vortex structure in samples with inclined CD's.[11] This description is sup-

ported by transport dc measurements carried out in nonirradiated twined $YBa_2Cu_3O_7$ crystals that suggest that correlated disorder plays an important role for all the field orientations.[12] On the other hand, sophisticate transport experiments[13,14] and recent measurements of the angular dependence of the ac susceptibility in similar samples[15,16] show a very complex scenario where the effect of the different sources of correlated pinning is still a matter of debate.

In order to clarify this scenario, in this work we study the angular dependence of the ac response of the vortex system at high temperature and low dc fields in crystals with a small density of CD's tilted relative to the c axis. In the first part we compare the results with those obtained for nonirradiated samples, with the scope to analyze which is the main source of pinning and whether the character of this pinning is correlated or random. In the second part we study exhaustively the dynamical response at different angles between the field H_{dc} and the tracks to evaluate the changes introduced in the dynamic diagram when the field is tilted with respect to the defects.

II. EXPERIMENTAL PROCEDURES

In this work we present ac susceptibility measurements performed on two twinned $YBa_2Cu_3O_7$ single crystals grown using a flux growth technique.[17] One of them (approximate dimensions $0.8\,mm \times 0.5\,mm \times 10\,\mu m$) was irradiated at room temperature with 291-MeV Au^{27+} ions at the TANDAR accelerator facility, with a dose-equivalent matching field $B_\phi \sim 700$ Oe at an angle $\theta_D = 30°$ from the c axis. The other one (approximate dimensions $0.5\,mm \times 0.5\,mm \times 15\,\mu m$) was used as a reference. In order to facilitate the comparison we selected both crystals from the same batch; they have identical critical temperature $T_c = 91.8$ K (defined as the onset of the ac transition at $H_{dc} = 0$ in the linear ac regime) and zero-field transition width $\Delta T_c \simeq 0.6$ K (defined as the range with nonzero dissipation in the same condition). In addition, the low irradiation dose used does not produce any measurable effect either in the critical temperature or in the transition width.

The complex ac susceptibility $\chi = \chi' + i\chi''$, was measured in an ac field $h_a e^{i\omega t}$ parallel to the c axis which is very homogeneous in the volume occupied by the sample. The amplitude h_a is varied from 5 mOe to 8 Oe and the frequency $f = \omega/2\pi$ from 300 Hz to 100 kHz. A uniform static field H_{dc} up to 1300 Oe is added. The ac coil setup and the sample (which are rigidly glued together) can be rotated with a precision of $\sim 1°$, allowing us to vary the angle θ between the c axis and H_{dc}. Measurements are performed in all the cases by slowly warming up the sample. Generally, several curves at various amplitudes h_a or at different angles θ were recorded during each temperature sweep. The scan in angle was always performed in the same direction to avoid backlash problems. All the curves of χ' and χ'' at each frequency are normalized by the same factor, corresponding to a total step $\Delta\chi' = 1$, with $H_{dc} = 0$. Other experimental details can be consulted in Ref. 10. Before introducing our results, we point out that throughout this paper two different angles are
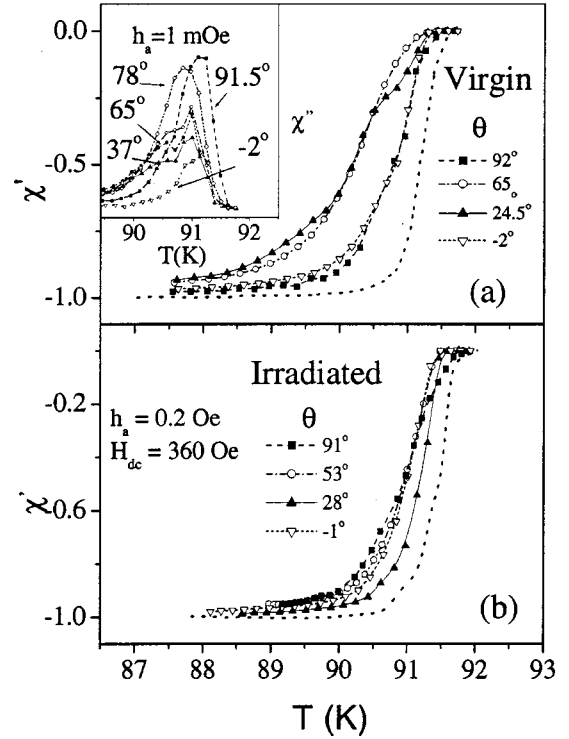

FIG. 1. (a) Temperature dependence of the out-of-phase component χ' of the ac susceptibility with the dc field oriented at various angles θ relative to the c axis in a nonirradiated sample. Inset: curves of the in-phase component χ'' as a function of T in the linear regime; a structure is present at intermediate angles. (b) Same in a sample irradiated with a matching field $B_\phi = 700$ Oe at $\theta = 30°$.

used: the angle θ between the c axis and H_{dc} and the angle $\varphi = \theta - \theta_D$ between H_{dc} and the tracks.

III. ANGULAR DEPENDENCE OF THE ac RESPONSE

In this section we will analyze the overall angular dependence of the susceptibility of the virgin and irradiated crystals. By comparing and contrasting the behavior of both samples, we will be able to identify several angular ranges where pinning is dominated by different mechanisms.

Figures 1(a) and 1(b) show some of the experimental χ' curves recorded as a function of temperature at different angles θ in both the virgin and irradiated crystals. All these curves were measured with $h_a = 0.2$ Oe and $H_{dc} = 360$ Oe. The zero-field transitions are also included as a reference (dotted curves). Comparison of both figures shows that when the direction of H_{dc} is close to the ab planes [curves for $\theta = 92°$ in Fig. 1(a) and $\theta = 91°$ in Fig. 1(b), shown with solid squares] the response of both samples is very similar. In contrast, at all other field orientations the irradiation produces a clearly visible upward shift of the $\chi'(T)$ curves, due to the additional pinning introduced by the CD's. Close to the defects [$\theta = 28°$, shown with solid up triangles in the Fig. 1(b)] pinning is drastically increased.

In the virgin sample, curves at intermediate angles [e.g., $\theta = 24.5°$, shown with solid up triangles in Fig. 1(a)] present
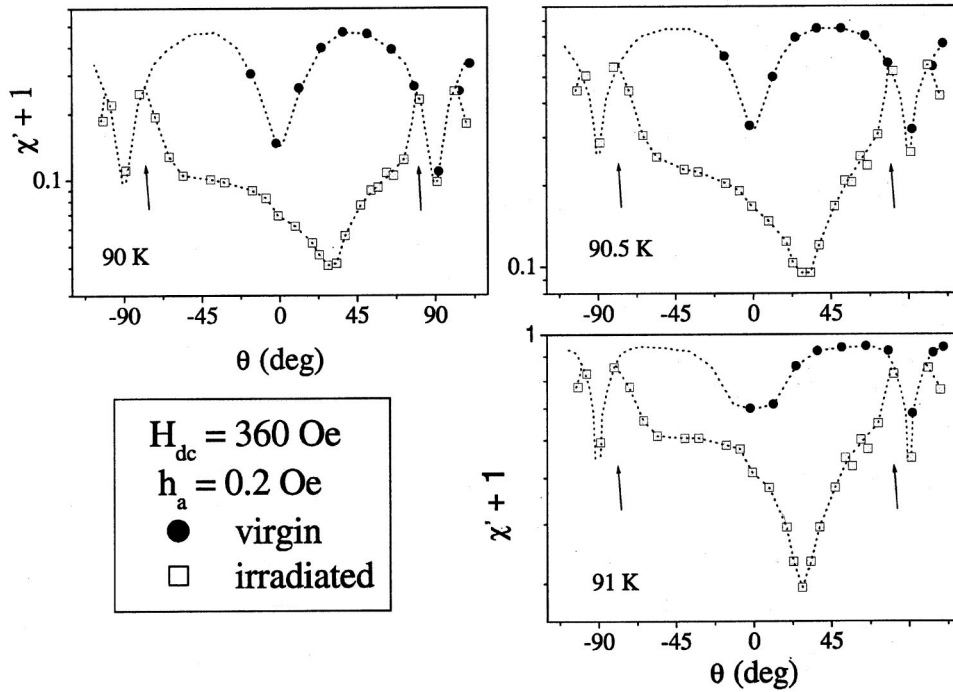
FIG. 2. Angular dependence of $\chi' + 1$ in the irradiated (open squares) and virgin sample (circles) at different temperatures. The dotted lines are guides for the eye (in the virgin sample it has been constructed from the expected symmetry relative to the c axis). In the irradiated sample, the symmetry is recovered at θ_{sim} (indicated by arrows). Beyond this angle both responses are very similar. All graphics are in semi-logarithmic scale.

a complicated structure. This characteristic structure extends to higher θ as h_a decreases, occurring up to around 75° in the linear regime, as can be seen in the inset of Fig. 1(a). A similar behavior has been reported in other works[16] and its origin is not clear. Careful experiments have shown that, in this angular region, thermomagnetic history must be taken into account. The sharp onset is generally associated with a first-order transition, while the cause of the previous decrease in $\partial\chi'/\partial T$ is unclear. Some works claim that it is due to a softening of the vortex lattice (peak effect),[18] while Ref. 16 states that it may be a consequence of the vanishing influence of twin boundaries with a consequent reordering of the vortex lattice. In any case, it can be seen that in the irradiated sample the structure disappears completely.

Data such as those shown in Fig. 1 can be used to build up curves of $\chi' + 1$ as a function of θ in both samples at fixed temperature. Figure 2 shows such curves at three different temperatures. Several features are apparent here. First, in the irradiated sample the original symmetry is broken [$\chi'(\theta) \neq \chi'(-\theta)$] by the presence of the tilted defects. This symmetry breaking occurs over a very large angular range; the symmetry is only recovered for $|\theta| \gtrsim \theta_{sim} \sim 75°$, signaled with arrows in the figure. Second, in the asymmetric range $|\theta| \lesssim \theta_{sim}$ the ac field screening is, at any temperature, larger than the one corresponding to the virgin sample. Third, beyond $|\theta_{sim}|$ the behavior of both samples is very similar. This last result suggests that the pinning properties in the vicinity of the ab planes are not significantly altered by the introduction of CD's. However, the ac response in that angle region is a strong function of θ, and a better angular resolution would be required to perform an accurate comparison.

The first obvious conclusion that arises from Fig. 2 is that pinning in the irradiated crystal is dominated by CD's over most field orientations. It is apparent that the CD's have a directional effect (i.e., they act as correlated pinning centers),

as they modify the original symmetry. This is true even when H_{dc} is almost perpendicular to the tracks, between −75° and −60°. Note also that, even in that angular region, the pinning due to the CD's is much more efficient than that present in the nonirradiated sample, as indicated by the much larger screening (smaller χ'). In the quadrant of positive θ angles (the right side of the figures), where the track direction is contained, the vortex pinning in the irradiated sample abruptly decreases around the θ_{sim} angle. Instead, in the left side the screening falls down at $\theta \sim -60°$, but the behavior of the nonirradiated sample is not recovered until 15° beyond this angle, at $\theta \sim -\theta_{sim}$. In Sec. IV B we will show that the angle in which the screening falls down (for this case about −60°) is h_a dependent and is a consequence of a change in the dynamic regime.

Figure 2 also shows that the response is not symmetric with respect to θ_D. This fact can be easily explained since the anisotropic character of the material and the presence of natural correlated defects (TB's and ab planes) should have an important role in the vortices accommodation. The observed correlated nature of the pinning implies that a fraction of the vortex lines remains accommodated in the CD's. However, the average segment length of the vortices pinned at defects is determined[11,19] by the competition between the pinning and elastic energies, both depending on the θ angle relative to the c axis.

The main point to emphasize from these measurements is that the angular region in which CD's act as correlated pinning centers is very large. It can also be noticed that, in the range of temperature of Fig. 2, $\theta_{sim} \sim 75°$ is nearly constant. This behavior is not consistent with the existence of an accommodation angle φ_A beyond which the correlated nature of the pinning should disappear, because at these high temperatures, a such angle is expected to be very narrow and to decrease fast with T. We have previously shown[11] from dc

magnetization measurements that, in a crystal with a higher density of CD's introduced at the same crystallographic orientation as in the present case, at temperatures about 60 K the symmetry relative to the c axis is recovered for $\theta_{\text{sim}} \sim 65°$. We also showed there that θ_{sim} slightly increases by increasing temperature, in opposition to the expected behavior for $\varphi_A(T)$. Our ac susceptibility results presented here are in compliance with this scenario and confirm the absence of an accommodation angle in twined $YBa_2Cu_3O_7$ crystals.

We now return to the situation for field directions close to the ab planes ($|\theta| > 75°$). The very similar behavior of both samples in this angular region suggests that the main pinning source is the same. A related feature is that, in the nonirradiated sample, the qualitative change in the linear response is observed very near $\theta \sim 75°$ [inset of Fig. 1(a)]. Beyond this angle, no structure is observed at any ac field. The above observations could be explained by assuming that θ_{sim} indicates the angle beyond which, for both the irradiated and virgin samples, the ab planes become the prevailing pinning centers.

IV. DYNAMIC REGIMES

In this section we present a detailed analysis of the ac response in the irradiated sample at various orientations of the dc field. The angles selected for this study are representative of the various angular regions observed in the previous section: H_{dc} aligned with the defects ($\theta \sim 30°, \varphi \sim 0$), H_{dc} at a very small angle relative to defects ($\theta \sim 34°, \varphi \sim 4°$), H_{dc} along the direction symmetric to the tracks relative to the c axis ($\theta \sim -30°, \varphi \sim -60°$), and H_{dc} in the angular region where the screening falls down ($\theta \sim -70°, \varphi \sim -100° \equiv 80°$). For comparison, we also include the response of the virgin sample for $\theta \sim 30°$. In all cases, the response at very low ac fields is linear [i.e., $\chi(T)$ is independent of h_a], and it becomes nonlinear above a threshold ac field $h_a^l(\theta, T)$. The experimental determination of h_a^l was discussed in detail in Ref. 10. In the following subsection we compare the results obtained in the linear regime for each one of the chosen angles, and later we analyze the nonlinear response.

A. Linear regime

In a linear regime χ' and χ'' are completely determined by the complex penetration depth $\lambda_{\text{ac}} = \lambda_R + i\lambda_I$ and the experimental geometry. In the last years, numeric solutions of $\chi(\lambda_{\text{ac}})$ for different geometries have been published.[20,21] In order to analyze our data, we chose to approximate our experimental situation to the one of a thin superconductor disk with a transverse ac field, and we used the solution proposed by Brandt for this case.[21] In this geometry, χ is only a function of the dimensionless parameter $\lambda_{\text{ac}}^2/(R\delta)$, where R and δ are the radius and thickness of the disk, respectively.

The vortex dynamics within the linear regime can be dominated by different types of forces. These different possibilities are parametrized by the ratio between the imaginary and real components of the penetration depth $\varepsilon = \lambda_I/\lambda_R$. In previous publications we have exhaustively discussed the physical meaning of the ε parameter.[9] If $\varepsilon \ll 1$, we are in the
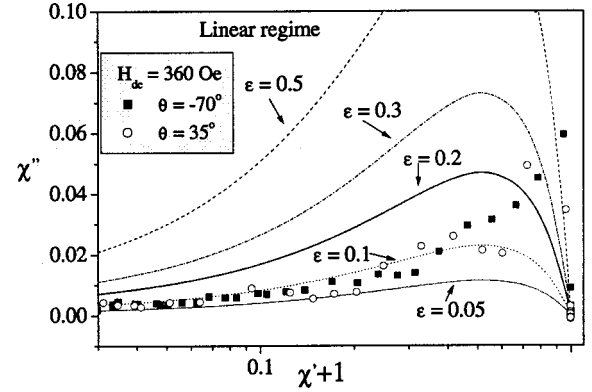

FIG. 3. Examples of experimental curves $\chi''(\chi' + 1)$ in the irradiated sample at two θ angles plotted in semilogarithmic scale. Lines are theoretical calculations for a disk in the linear regime corresponding to different values of $\varepsilon = \lambda_I/\lambda_R$. In all cases, below a certain temperature there is a small ε indicative of a Campbell regime.

presence of a Campbell regime, in which elastic pinning forces dominate. The pinning force can be expressed as $F_p(r) = -\alpha_L u(r)$, where α_L is the average curvature of the pinning potentials, or Labusch constant, and $u(r)$ is the average displacement of the vortices at the r position. In the other limit $\varepsilon = 1$, dissipative terms dominate and the system is Ohmic with a real resistivity. When both pinning and dissipative forces contribute significantly to the response, ε takes intermediate values.

The fact that, for a given geometry, the function $\chi''(\chi')$ in the linear regime depends only on ε can be used to determine this important parameter. To illustrate the procedure, in Fig. 3 we show experimental points of χ'' vs $\chi' + 1$ of the irradiated sample for two of the chosen angles, together with theoretical curves calculated for different values of ε in a disk in the linear regime. We observe that below a certain temperature (i.e., below a certain value of χ', about $\chi' + 1 \sim 0.3$ in the particular cases shown in Fig. 3), ε remains small, indicating a Campbell regime. We corroborated that this is the case for each one of the chosen directions of H_{dc}; that is, a Campbell regime is always present at low enough temperature.

In the Campbell regime ($\varepsilon \ll 1$), to first order in ε the screening χ' depends only on λ_R; therefore, $\lambda_R^2(\chi')$ can be easily obtained.[9] Moreover, in this limit $\lambda_R^2 = \lambda_L^2 + \lambda_C^2$, where λ_L^2 is the square of the London penetration length and $\lambda_C^2 = (\phi_0 B/4\pi\alpha_L)$ is the square of the Campbell penetration depth. In this expression ϕ_0 is the flux quantum and α_L is the Labusch constant per vortex unit length. It can be seen from the last expression that, if α_L is independent of B (Campbell regime of individual vortices), λ_C^2 will be proportional to B.

To analyze the B dependence of α_L, measurements for several values of dc fields along the chosen directions in the linear regime have been performed and the corresponding $\lambda_R^2(\chi')$ have been calculated. We have observed qualitative differences in the behavior in the various angular ranges. The results are summarized in Figs. 4 and 5.
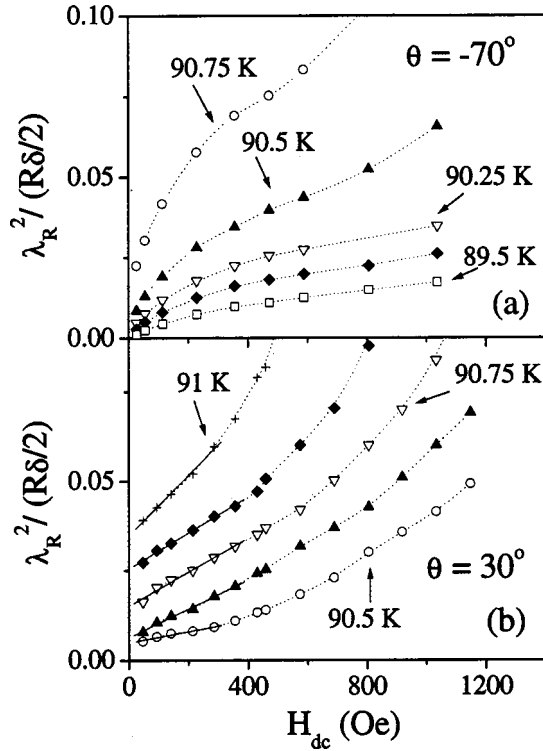
FIG. 4. Field dependence of the square of the dimensionless linear real penetration depth at different temperatures *measured with an* $h_a = 5$ mOe. (a) H_{dc} in a direction forming a large angle φ with defects. (b) H_{dc} parallel to defects.
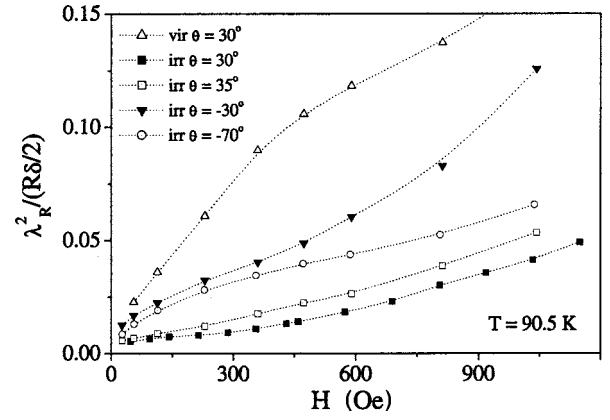

FIG. 5. Field dependence of the square of the dimensionless linear real penetration depth in the irradiated sample at a fixed temperature for different angles θ. A curve of the virgin sample at the same temperature is also shown. All curves were measured with an $h_a = 5$ mOe.

Figure 4 shows the calculated dimensionless $\lambda_R^2/(R\delta/2)$ as a function of the dc field for different temperatures in the case of an angle $\theta = -70°$, far away from the defects [Fig. 4(a)] in comparison with those obtained with the field parallel to tracks [Fig. 4(b)]. As we have shown in previous publications,[9,10] when the field is aligned to defects, λ_R^2 is linear with B up to $B \simeq B_\phi/2 (\sim 400 \text{ Oe})$, pointing to the presence of a Campbell regime with a pinning force independent of dc field, with vortices individually pinned by the columnar defects. For higher dc fields, there is an increase in the ratio $\lambda_R^2/B \sim \lambda_C^2/B \propto \alpha_L^{-1}$, due to the decrease of α_L as the effective pinning becomes dependent on the lattice interactions. We have also shown that, for samples with B_ϕ well above our maximum accessible H_{dc}, the linearity $\lambda_C^2 \propto B$ is maintained in our whole H_{dc} range. The fact that the linear slope increases with temperature arises from the weakening of the individual pinning force (i.e., α_L decreases with T). At $\theta = -70°$ the response is completely different: $\lambda_R^2(B)$ begins with a larger slope (i.e., a lower α_L) and, for low fields, shows a negative curvature (i.e., α_L increases with field); for higher fields, it develops a slightly positive curvature.

Let us now analyze the behavior at intermediate angles and see how the response in the linear regime compares with that observed in the virgin sample. In Fig. 5 various curves of $\lambda_R^2(B)$ for the chosen values of θ are compared at $T = 90.5$ K. We see that the qualitative $\lambda_R^2(B)$ behavior observed when B is aligned to the defects [Fig. 4(b)] still holds if the field is tilted by a few degrees ($\theta = 34°$), but it changes

notably for greater tilts. The behavior is also very different in the nonirradiated sample. In the last two cases, no linear dependence in λ_R^2 vs B at low fields is observed, indicating that a Labusch constant independent of field does not exist. (The fact that in these cases α_L decreases with increasing B is noteworthy, as collective pinning theories never predict this behavior; its physical meaning is an open question.) It can also be seen that when the dc field is aligned with the defects λ_C^2 is much lower than for either angles far away (4 or 5 times) or for the nonirradiated sample (10 times). For fields higher than $B_\phi/2$, the ratio between the Campbell lengths in different orientations decreases.

Furthermore, we observe that the response at $\theta = -30°$ in the irradiated sample is different from the response observed at $\theta = 30°$ in all the range of measured fields; this means that up to $H_{dc} \approx 2B_\phi$ the presence of defects is still important. A noteworthy result is that, for low dc fields, the responses at $-70°$ and $-30°$ are very similar. Near $H_{dc} = B_\phi/2$, the curve for $\theta = -30°$ starts to increase more swiftly, and both responses can be clearly distinguished. This fact indicates that even at an angle $\varphi \sim -60°$ from the tracks direction the occupation of defects play an important role.

The above experimental results can be qualitatively understood as follows. In the first part of this work, we conclude that vortices are partially accommodated in the defects for all the chosen angles. The restitutive constant α_L is higher in the vortex segments that are accommodated into the columnar defects. For this reason, while the Campbell regime remains individual, the average Labusch constant increases with the length of pinned segments, i.e., when the angle φ (relative to the defects) decreases. For large φ the situation is more complex: First, the fraction of each vortex pinned by the tracks is very small (it can be seen that α_L for the nonirradiated sample at $30°$ is just half the value observed at $-30°$ in the irradiated sample). Moreover, the pinning force for small displacements is comparable to that induced by neighbor vortices and α_L is no longer independent of B.
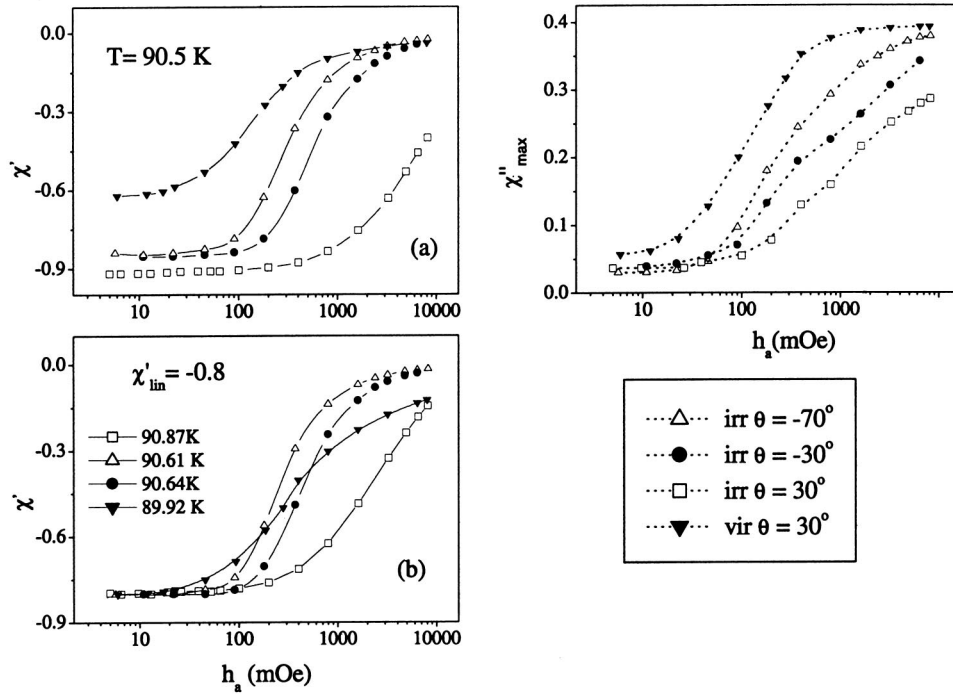
FIG. 6. Linear and nonlinear behavior at different angles θ as a function of the ac field. (a) Comparison of $\chi'(h_a)$ curves at the same temperature. (b) Comparison at the same linear real penetration depth and (c) maximum of the dissipative component $\chi'(T)$. Symbols correspond to the three panels and all graphics are in semilogarithmic scale.

B. Nonlinear response

Measurements in all the available range of h_a have been performed. The first notable observation is that, in the non-linear regime, the angular dependence of the ac response is much more pronounced. For large angles relative to the columnar defects direction, as soon as the linear behavior is lost, the $\chi(T)$ curves get wider in temperature and the dissipation peaks notably increase. These facts are summarized in Fig. 6, where the nonlinear behavior at different angles and their comparison with the nonirradiated sample are shown. In Fig. 6(a), various $\chi'(h_a)$ curves at the same temperature (90.5 K) for different angles are plotted, while in Fig. 6(b) all the curves included have the same λ_R (and therefore they were obtained at different temperatures). In Fig. 6(c) the dependence of the maximum of the dissipative component $\chi''_{max}(h_a)$ is shown.

It can be observed that the ac field h_a^l at which loss of linearity occurs is lower when the pinning due to the CD's is less efficient: in the nonirradiated sample (solid down triangles in the figure), h_a^l is almost one order of magnitude lower than in the case of the irradiated sample with field aligned to defects (open squares in the figures). When H_{dc} is aligned to the CD's, the departure from linearity is smooth, while for large φ angles (solid circles and open up triangles in the figures) the departure from linearity is much more abrupt.

As we have reported in previous works,[9,10] when H_{dc} is aligned with the tracks the maximum of $\chi''(T)$ for the highest h_a is similar to the value expected in a critical-state regime ($\chi''_{max} \sim 0.24$ for a disk in transversal geometry). Figure 6(c) shows that this fact does not hold for large φ angles: for relatively small ac fields χ''_{max} overcomes the characteristic maximum of the critical state and, for the highest fields, approaches the expected values for the ohmic regime (

$\chi''_{max} \sim 0.44$ for a disk in transversal geometry). This behavior is still more notable in the nonirradiated sample. Consistently with the last observation, for those high ac fields the dependence of χ on h_a decreases tending to a new linear regime.

To check this last remark, in Fig. 7 we compare experimental points of χ'' vs $\chi'+1$ obtained at different angles at $h_a \sim 6.4$ Oe, with those calculated for a disk both in the Bean critical state (solid line in the figure) and in the Ohmic regime (dashed line). While in the irradiated sample the response at $\theta = 30°$ is similar to the expectation for a critical state, for angles far away from the defects it tends to the Ohmic behavior. Notice that, as well as χ''_{max} increases, $\chi'(\chi''_{max})$ also tends to the expected value in a linear Ohmic regime.

As another test to close this picture, we tried to check whether a critical-state regime is established or not, making use of the experimental method presented in Ref. 10. We will not explain this method in detail here. Essentially, it consists in building up an experimental critical-state characteristic length $\Lambda_c(\chi'(h_a,T)) \propto h_a/J_\omega(T)$ (where J_ω is the frequency-dependent current density established in the critical state) and then to check the consistency of the resulting function $\Lambda_c(h_a)$ at each temperature. A critical state is established if, at constant T and ω, Λ_c turns out to be proportional to h_a. The typical result in the case of vortices aligned to defects is illustrated in Fig. 8(a) where plots of $\Lambda_c(h_a)$ for different temperatures are shown. Above an $h_a^c(T)$ (signaled by arrows in the figure), Λ_c is proportional to h_a. Figure 8(b) shows the result of the same procedure applied to data obtained at $\theta = -70°$. Whereas in the case of H_{dc} aligned with the tracks a consistent function was obtained (i.e., the existence of a critical-state regime was proved), at large φ a satisfactory solution was not attained.
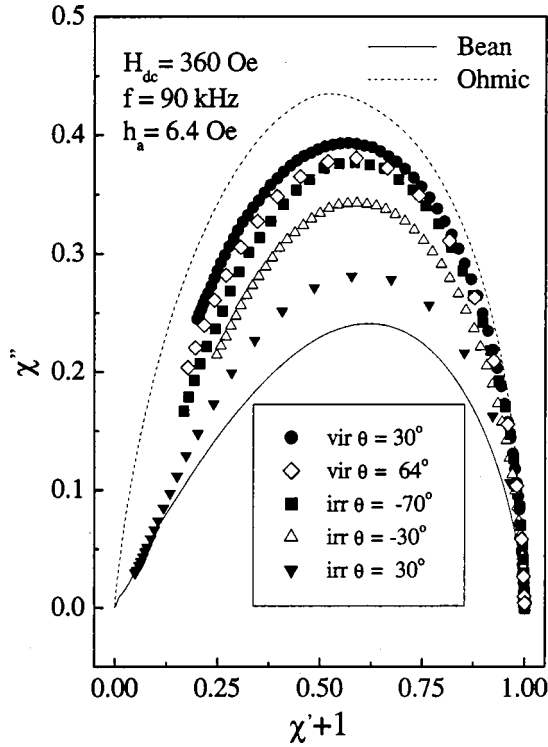
FIG. 7. Experimental curves $\chi''(\chi')$ at a large $h_a = 6.4$ Oe in the irradiated and virgin sample for various angles. Lines are the theoretical calculation for a disk in an Ohmic regime (dashed line) and in a Bean critical state (solid line).

FIG. 8. Test to prove the existence of a critical regime, i.e., the consistency of the function $\Lambda_c(\chi') \propto h_a / J_\omega(T)$. (a) When the dc field is aligned with the defects, Λ_c is proportional to h_a above $h_a^c(T)$ (signaled by arrows). (b) At large angles φ, there is not a good solution. Plots are in logarithmic scale.

A possible explanation for this behavior is the following: When φ is large, the effective critical current density J_ω is much lower than in the case in which H_{dc} is aligned with the tracks. In fact, it is so much reduced that a critical state cannot be established: as soon as the linearity is lost and the vortex displacements become mainly determined by creep mechanisms across the pinning centers, the ac field penetration length increases very much and becomes comparable to the flux-flow skin depth. In this condition, a nonlinear regime in which pinning forces, activated mechanisms, and viscous losses contribute significantly to the vortex motion is established.

Finally, another interesting consideration arises from Fig. 6, as it allows us to reanalyze the angular dependence of $\chi(\theta)$ previously shown in Fig. 2. The angle beyond which there is an abrupt increase in the ac field penetration in the left side of Fig. 2 ($\theta \approx -60°$) corresponds to the angle for which, at the particular ac field value $h_a = 0.2$ Oe, the system changes from a nearly linear regime to a nonlinear one. This fact can be easily verified crossing the curves $\chi'(h_a)$ at $h_a = 200$ mOe in Fig. 6(a). By performing the same procedure at lower h_a we can observe that, if angular measurements were made at lower ac fields, a smooth angular dependence would extend to orientations closer to the ab planes. On the other hand, if we perform the procedure for $h_a = 400$ mOe, the abrupt increase of ac field penetration will appear before $\theta = -30°$. For even higher values of h_a, the region drastically affected by the CD's will only involve the peak close to the defects, as has been reported previously.[19] From all this
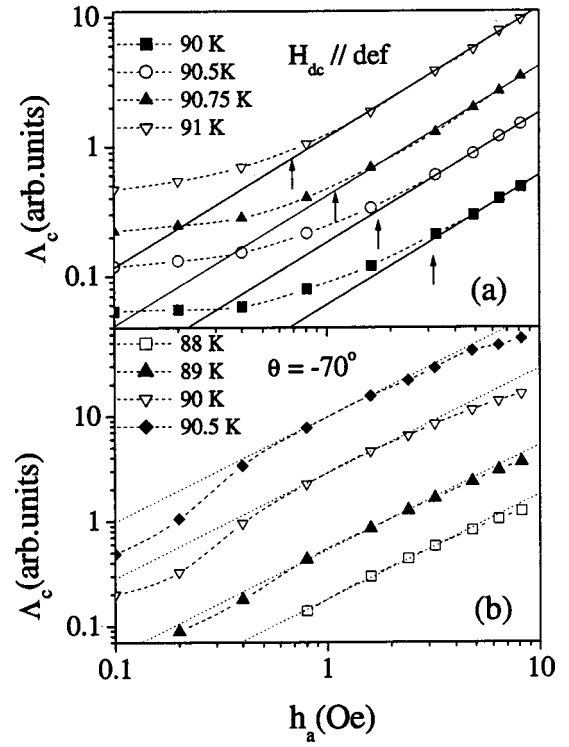
considerations, we point out that the apparent angular region notably affected by the CD's is h_a dependent. Thus results arising from studies carried out using only one ac amplitude should be interpreted with caution.

V. CONCLUSIONS

From the comparison between the angular dependence of the ac susceptibility in irradiated and virgin samples, we conclude that columnar defects are the main source of correlated pinning even when the angle φ between them and the dc field is large. This fact is not consistent with the presence of an accommodation angle going to zero when approaching the liquid transition.

We have also shown that the width of the angular region in which the screening is notably increased by defects (strong peak around the tracks direction) is related to an abrupt change in the dynamic regime and its limit depends on the amplitude of the ac field. The linear regime limit angle coincides with a qualitative change in the behavior of the virgin sample. Beyond this limit angle, the main sources of pinning in the irradiated and virgin samples seem to be the same. Our results are consistent with a predominance of the intrinsic pinning due to ab plane in this region. However, due to the strong angular dependence of the ac response in the vicinity of the ab planes, it is clear that a similar study with a better resolution should be necessary to confirm the last conclusion.

For small enough ac fields, a Campbell regime is established in all cases. We observe important qualitative differences in the pinning potential for directions close and far away from defects. For low φ, the Labusch constant is independent of field up to $H_{dc} \sim B_\phi/2$ and decreases with increasing φ. This behavior is consistent with a picture in which vortices are individually pinned by the columnar defects: the average restoring force is proportional to the vortex fraction pinned in the defects at each angle. At larger φ values the response is completely different: collective effects and other pinning sources have to be taken into account. However, in all cases the influence of defects is still important up to the highest applied field $H_{dc} \approx 2B_\phi$.

The departure from linearity is much more abrupt when the field is far away from the tracks. In these cases, no critical state is established in the frequency range of our measurements. For the highest ac fields the behavior approaches an Ohmic regime.

Finally we would like to remark the last conclusion about the analysis of the angular dependence of the ac response in vortex systems: from the above results, it is clear that angular measurements performed using only one ac field, without characterizing the dynamic regimes involved, may be erroneously interpreted.

*Corresponding author. Electronic address: gpmm@bigfoot.com

[1] G. Blatter, M. V. Feigel'man, V. B. Geshkenbein, and V. M. Vinokur, Rev. Mod. Phys. **66**, 1125 (1994).

[2] L. Civale *et al.*, Phys. Rev. Lett. **67**, 648 (1991); J. Thompson *et al.*, Appl. Phys. Lett. **60**, 2306 (1992); M. Konczykowski *et al.*, Phys. Rev. B **44**, 7167 (1991); W. Gerhauser *et al.*, Phys. Rev. Lett. **68**, 879 (1992); R. C. Budhani *et al.*, *ibid.* **69**, 3816 (1992).

[3] M. Konczykowski, V. Vinokur, F. Rullier-Albenque, Y. Yeshurun, and F. Holtzberg, Phys. Rev. B **47**, 5531 (1993); M. Konczykowski, Physica C **209**, 247 (1993); J. R. Thompson, L. Krusin Elbaum, L. Civale, G. Blatter, and C. Feild, Phys. Rev. Lett. **78**, 3181 (1997); L. Civale, Supercond. Sci. Technol. **10**, A11 (1997) and references therein.

[4] D. R. Nelson and V. M. Vinokur, Phys. Rev. Lett. **68**, 2398 (1993); Phys. Rev. B **48**, 13 060 (1993).

[5] L. Krusin-Elbaum, L. Civale, G. Blatter, A. Marwick, F. Holtzberg, and C. Feild, Phys. Rev. Lett. **72**, 1914 (1994).

[6] W. Jiang, N.-C. Yeh, D. S. Reed, U. Kriplani, A. D. Beam, M. Konczykowski, T. A. Tombrello, and F. Holtzberg, Phys. Rev. Lett. **72**, 550 (1994).

[7] L. Krusin-Elbaum, L. Civale, J. R. Thompson, and C. Feild, Phys. Rev. B **53**, 11 744 (1996).

[8] L. Civale, G. Pasquini, P. Levy, G. Nieva, D. Casa, and H. Lanza, Physica C **263**, 389 (1996).

[9] G. Pasquini, P. Levy, L. Civale, G. Nieva, and H. Lanza, Physica C **274**, 165 (1997).

[10] G. Pasquini, L. Civale, H. Lanza, and G. Nieva, Phys. Rev. B **59**, 9627 (1999).

[11] A. Silhanek, L. Civale, S. Candia, G. Nieva, G. Pasquini, and H. Lanza, Phys. Rev. B **59**, 13 620 (1999).

[12] E. H. J. Morrè, Ph.D. thesis, Instituto Balseiro, 1997; E. H. J. Morè *et al.*, Phys. Lett. A **233**, 130 (1997).

[13] D. Lopez, L. Krusin-Elbaum, H. Safar, V. Vinokur, A. D. Marwik, J. Z. Sun, and C. Field, Phys. Rev. Lett. **75**, 3525 (1997).

[14] H. Pastoriza, S. Candia, and G. Nieva, Phys. Rev. Lett. **83**, 1026 (1999).

[15] G. A. Jorge and E. Rodriguez, Phys. Rev. B **61**, 103 (2000).

[16] S. O. Valenzuela and V. Bekeris, Phys. Rev. Lett. **84**, 4200 (2000).

[17] F. de la Cruz, D. Lopez, and G. Nieva, Philos. Mag. B **70**, 773 (1994).

[18] W. De Sorvo, Rev. Mod. Phys. **36**, 90 (1964); W. K. Kwok, J. A. Fendrich, C. J. van der Beek, and G. W. Crabtree, Phys. Rev. Lett. **73**, 2614 (1994).

[19] J. A. Herbsommer, J. Luzuriaga, L. Civale, G. Nieva, G. Pasquini, H. Lanza, and P. Levy, Physica C **304**, 112 (1998).

[20] Th. Herzog, A. A. Railovan, P. Ziemann, and E. H. Brandt, Phys. Rev. B **56**, 2871 (1997); E. H. Brandt, Supercond. Sci. Technol. **11**, 921 (1998).

[21] E. H. Brandt, Phys. Rev. B **49**, 9024 (1994); **50**, 4034 (1994); **50**, 13 833 (1994).